ACS APPLIED MATERIALS & INTERFACES

Research Article

www.acsami.org

Compartmentalized Multilayer Hydrogel Formation Using a Stimulus-Responsive Self-Assembling Polysaccharide

Yuan Xiong,[†] Kun Yan,[†] William E. Bentley,[‡] Hongbing Deng,[†] Yumin Du,[†] Gregory F. Payne,*[,†,‡] and Xiao-Wen Shi*[,†]

[†]School of Resource and Environmental Science, Hubei Biomass-Resource Chemistry and Environmental Biotechnology Key Laboratory, Wuhan University, Wuhan 430079, China

[‡]Institute for Bioscience and Biotechnology Research and Fischell Department of Bioengineering, University of Maryland, College Park, Maryland 20742, United States

ABSTRACT: Polymeric systems that self-assemble through strong noncovalent bonds form structures that are highly dependent on the spatiotemporal sequence of cues that trigger self-assembly. Here, we prepared capsules with a semipermeable alginate−chitosan polyelectrolyte membrane that encapsulates a solution of the pH-responsive self-assembling aminopolysaccharide chitosan. Immersion of these capsules in a basic solution triggers gelation of the capsule contents, and the details of the gel-inducing treatment dramatically affect the final structure of the gelled compartment. Specifically, we show that the sequential transfer of the capsules between the base and water can generate multilayer hydrogel structures, with the thickness of each layer being controlled by the base concentration and immersion times. We further demonstrate that these multilayer hydrogels can serve as templates for the synthesis of iron oxide particles with a complex internal structure (i.e., with a multilayer internal structure). This work demonstrates the ability to enlist the stimulus-responsive self-assembling properties of biological polymers to create materials with complex structures.

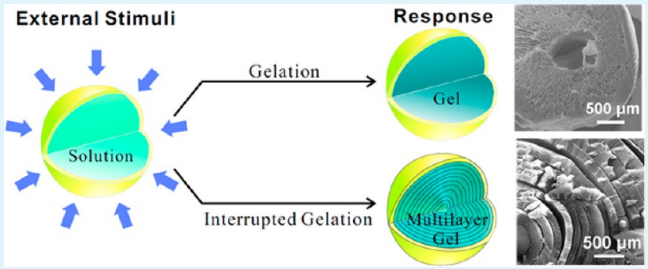

KEYWORDS: *chitosan, external stimuli, interrupted gelation, multilayer, self-assembly*

INTRODUCTION

Polymers possess considerable conformational freedom and can undergo transitions (e.g., coil to globule) that allow them to display diverse structures and properties. However, this conformational freedom makes *de novo* design and prediction challenging.[1] For instance, a globular protein tends to fold into a single thermodynamically preferred conformation, yet we have limited capabilities to predict this "native" conformation from the amino acid sequence. This limitation in predictive ability is exacerbated when multiple polymer chains undergo hierarchical self-assembly to generate specific material properties.[2]

While the protein folding problem illustrates the limitations of our predictive abilities, it also illustrates that biological polymers often contain the requisite information to self-assemble into useful structures without our complete understanding.[3,4] Interestingly, when self-assembly results in the formation of strong noncovalent bonds, then the final structure and properties are controlled not only by thermodynamics but also by the spatiotemporal sequence of cues that trigger self-assembly.[5−7] Here, we demonstrate that complex structures can be generated by spatially localizing biopolymer self-assembly and temporally controlling the cues that trigger self-assembly.

Scheme 1 illustrates our experimental system. We start by dropping a solution of the aminopolysaccharide chitosan into a solution containing the acidic polysaccharide alginate. A stable polyelectrolyte membrane (PEM) forms at the interface between these two aqueous solutions.[8] This PEM serves as a semipermeable barrier that spatially localizes (i.e., compartmentalizes) chitosan while allowing diffusion of permeable species across the membrane. As illustrated in Scheme 1, chitosan is capable of pH-responsive self-assembly.[9] At low pH, chitosan's primary amines are protonated, making it a water-soluble cationic polyelectrolyte. At high pH, chitosan's amines are deprotonated and the neutral form can self-assemble into a three-dimensional hydrogel with noncovalent cross-links formed from crystalline network junctions.[10] Because chitosan's gelation involves the formation of strong noncovalent bonds, the structure and properties of the resulting gel significantly depend on the spatiotemporal sequence of cues that are imposed to trigger its self-assembly (i.e., to induce its sol−gel transition). Here, we induce gelation of the capsule contents by the addition of base to the external solution and demonstrate that the conditions used to induce this gelation dramatically affect the internal structure of the emergent chitosan hydrogel.

Received: December 3, 2013
Accepted: January 28, 2014
Published: January 28, 2014

   dx.doi.org/10.1021/am405544r | *ACS Appl. Mater. Interfaces* 2014, 6, 2948−2957

Scheme 1. Formation of a Capsule That Can Respond to Externally Imposed Stimuli[a]

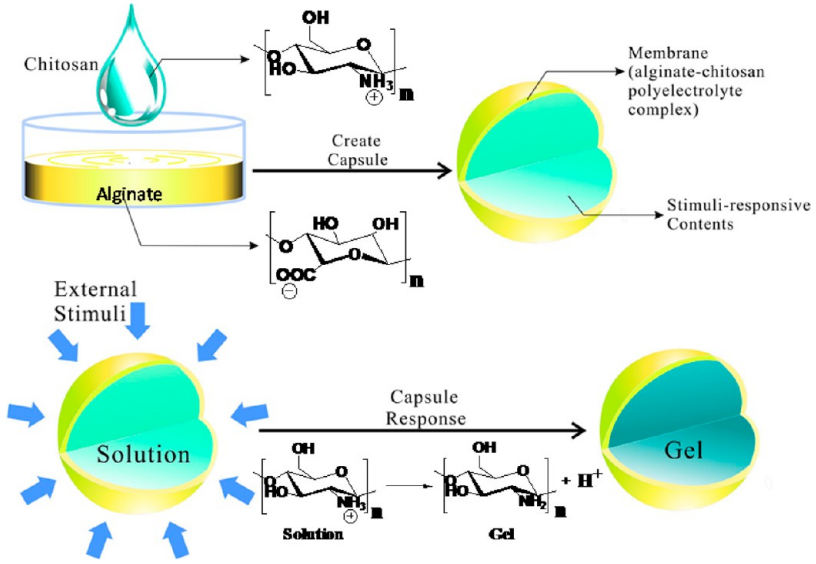

[a]An alginate−chitosan polyelectrolyte membrane (PEM) is formed to compartmentalize the chitosan solution, which can be triggered to undergo gel formation in response to externally imposed stimuli (i.e., base).

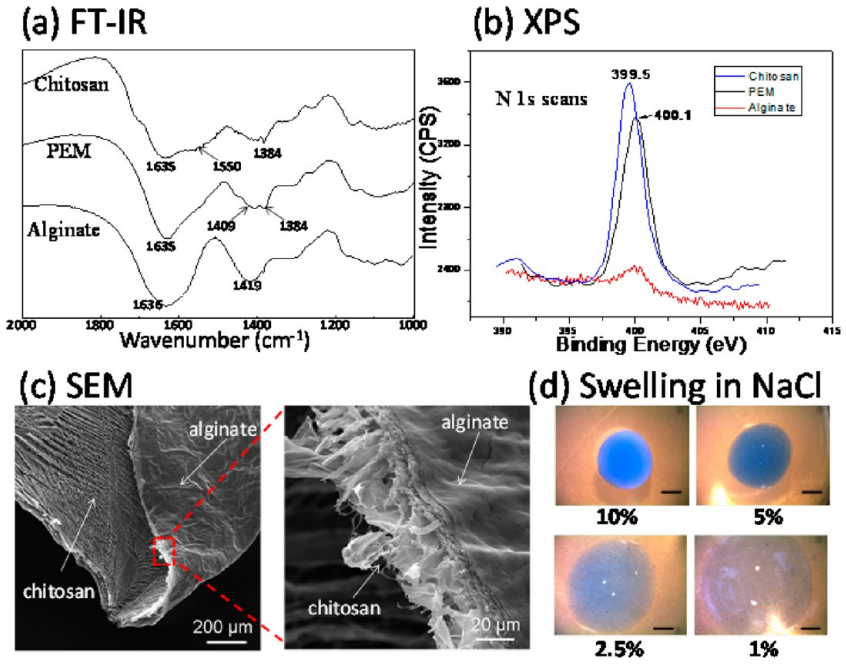

Figure 1. Characterization of an alginate−chitosan polyelectrolyte membrane (PEM). (a) FT-IR spectra of chitosan, alginate, and the PEM. (b) XPS N 1s narrow scans of chitosan, alginate, and the PEM. (c) Scanning electron microscopy images of the PEM. (d) Optical images show the chitosan-containing capsules swell when the NaCl concentration is decreased.

RESULTS

Polyelectrolyte Membrane. We first provide chemical evidence of the formation of a PEM between chitosan and alginate. For this, we added a single drop of a chitosan solution [4% (w/v), pH 4.0] to an alginate solution (2%) and incubated the capsule for 4 h (the solution was not stirred to ensure the spherical capsule was not deformed). After incubation, the capsule was removed from the alginate solution and rinsed with water. Visually, a thin transparent membrane was observed to encapsulate the fluid-filled capsule. The capsule was then pierced to release the contents, and the membrane was collected, rinsed, and dried for further analysis.

The alginate−chitosan PEM was first analyzed by Fourier transform infrared spectroscopy (FT-IR) as shown in Figure 1a. A chitosan control membrane was prepared by vacuum drying a chitosan solution (dissolved in 2% acetic acid). The spectrum for this control shows two adjacent peaks at 1635 and 1550 cm^{-1}, which demonstrates partial protonation of amine groups in the chitosan membrane.[11] An alginate control membrane was prepared by vacuum drying an aqueous solution of sodium alginate. The spectrum of the alginate membrane shows two strong peaks at 1636 and 1419 cm^{-1} that can be assigned to the

dx.doi.org/10.1021/am405544r | ACS Appl. Mater. Interfaces 2014, 6, 2948−2957

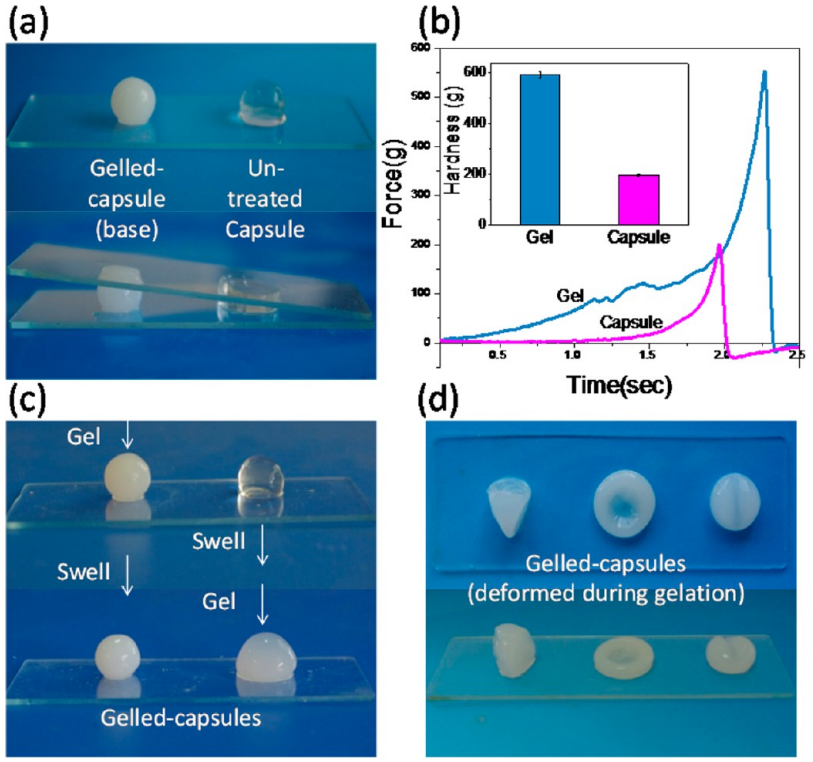

Figure 2. Evidence that externally imposed stimuli can induce the localized gelation of chitosan within the capsule. (a) Gelation of the internal contents confers opacity and elasticity to the capsule. (b) Mechanical measurements show the gelled capsules are stronger (as measured by hardness using a texture analyzer). (c) The size of the gelled capsules depends on the processing pathway. The capsule at the left was gelled prior to immersion in water, while the capsule on the right was gelled after immersion in water to allow swelling. (d) The shape of the gelled capsule can be altered by imposing deforming forces at the time that gelation is induced.

antisymmetric and symmetric stretches, respectively, of $-CO_2^-$ groups.[12] The absence of the peak at 1710 cm^{-1} also suggests the carboxylate groups are deprotonated. The spectrum from the alginate–chitosan PEM shows an overlap of carboxylate and $-NH_3^+$ in the range of 1400–1650 cm^{-1} as well as a $-CH_3$ band at 1384 cm^{-1}. These FT-IR results provide chemical evidence that both chitosan and alginate are present in the capsule PEM.

The PEM was further examined by X-ray photoelectron spectroscopy (XPS). Figure 1b shows N 1s narrow scans for the PEM and comparable controls from chitosan and alginate membranes. Because alginate lacks elemental N, there is little to no signal in this region of the spectrum for the alginate control. The N 1s spectrum for the chitosan control displays a peak at 399.5 eV, which is assigned to the primary amine that indicates that the amine groups are deprotonated during the drying process (e.g., acetic acid is evaporated). The shift in this peak to 440.1 eV for the PEM indicates that some of chitosan's amines are protonated presumably because of interactions with the deprotonated carboxylate groups of alginate. These XPS results provide chemical evidence that the PEM was formed by electrostatic interactions between chitosan and alginate.

The micromorphology of the capsule membrane was observed using scanning electron microscopy (SEM). The SEM images in Figure 1c reveal that the membrane has a smooth outer surface (alginate-facing), while the inner surface (chitosan-facing) is rough. Interestingly, this microstructure appears similar to layers and interfaces generated with polysaccharide–peptide systems.[13,14] The thickness of the capsule membrane is estimated to be 10 μm.

Next we demonstrate that the alginate–chitosan membrane possesses semipermeable properties. For this, we dissolved dextran blue in the chitosan to provide a high-molecular mass (2×10^6 Da) and readily observable marker. Capsules were prepared by dropping this aqueous dextran–chitosan mixture into a sodium alginate solution. After incubation, the capsules were removed and then immersed in solutions containing varying concentrations of NaCl for 8 h. The photograph at the top left in Figure 1d shows that incubation in 10% NaCl resulted in a small capsule with a bright blue color. This indicates that the dextran blue was retained within the capsule with little blue appearing in the surrounding salt solution (note that the photo shows both the capsule and surrounding transparent NaCl solution). The remaining photographs in Figure 1d show that incubation in lower concentrations of salt resulted in swelling of the capsules. Despite the swelling, a large proportion of the dextran blue was retained within the capsule over this 8 h incubation. These results indicate that the alginate–chitosan PEM is semipermeable as water can pass into the membrane (for swelling), while the high-molecular mass dextran blue is retained within the capsule. We should note that more extensive studies would be required to thoroughly characterize the membrane's semipermeability and to determine how these properties depend on the conditions used to prepare the capsules as well as the extent of swelling.

Gelation of the Capsule Contents. We next demonstrate that base added to the external environment can induce the chitosan solution compartmentalized within the capsule to undergo gelation. Experimentally, we prepared capsules by dropping the chitosan solution (4% chitosan dissolved in 2% acetic acid) into an alginate solution (2%) and incubated these

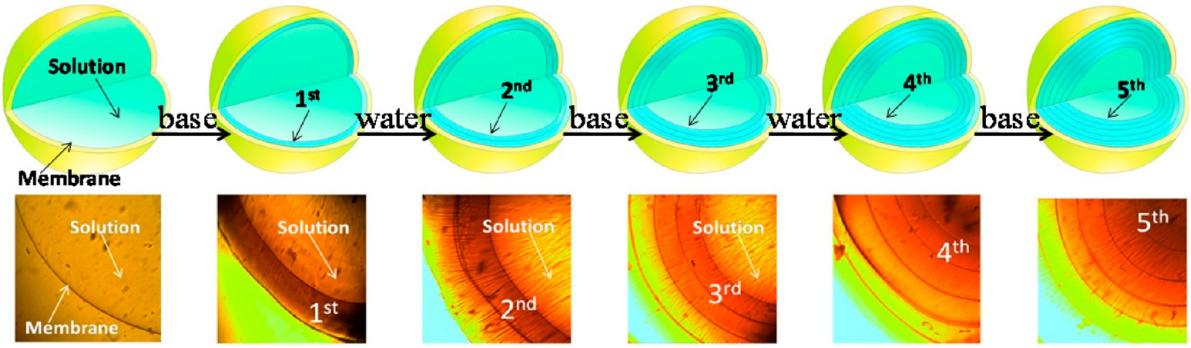

Figure 3. *In situ* observations of multilayer structure generation. The top panel shows the schematic illustrating that transfer steps between water and base or base and water generate an interface that demarcates the individual layers. The bottom panel shows photomicrographs obtained during the individual steps in the gel-forming process.

capsules for 4 h to allow the PEM to harden. After being rinsed with water, one capsule was immersed in base (5% NaOH) for 10 min to induce gelation of the contents. The top photograph in Figure 2a shows that the base treatment resulted in the capsule becoming opaque compared to the untreated control capsule that was not incubated in base. The bottom photograph in Figure 2a indicates that the base treatment also resulted in a more rigid capsule that was not deformed by the weight of the glass slide. Both observations are consistent with the explanation that an external pH change triggers a localized sol−gel transition of the capsule contents.

To provide a more quantitative comparison, we used a texture analyzer to measure the mechanical properties of gelled and untreated capsules. Experimentally, individual gelled or untreated capsules were compressed (2 mm/s) to a final deformation of 90%, and the force of deformation was measured. During this deformation, both the gelled and untreated capsules were observed to break. As indicated by the curves in Figure 2b, stronger forces were required to deform the gelled capsules. The maximal force during deformation is defined as the hardness (typically reported in units of grams), and these values are shown in the inset of Figure 2b. These values further indicate that the gelled capsules are considerably stronger than the untreated capsules containing a liquid core. These measurments show that the external pH change hardens the capsules, consistent with a pH-induced gelation of the capsule contents.

In a separate study, we compared the response of capsules to swelling and gelling conditions when they were applied in a different sequence. In this experiment, we created capsules as described above and exposed one to gel-inducing conditions as illustrated by the top photograph in Figure 2c. Both the gelled and ungelled capsules were then transferred to water and incubated for 10 min. During this water incubation, the ungelled capsule was observed to swell considerably. After 10 min, the external water solution was carefully replaced with a base solution, and the contents of the swollen capsule were allowed to undergo gelation for 10 min. The bottom photograph in Figure 2c compares the two gelled capsules from this experiment. The first conclusion from this experiment is that despite the extensive swelling of the membrane, chitosan is retained within the capsule and can undergo subsequent gelation. The second conclusion is that the obvious difference in the shapes of the two gelled capsules is consistent with gelation resulting from strong noncovalent bonds. Despite both capsules being exposed to the same final conditions, the initially gelled capsule did not swell (i.e., the pathway taken to gelation, and not thermodynamics, controlled the size and shape of the gelled capsules).

In the previous experiment, we induced gelation of the capsule compartment after it had been deformed by internal swelling forces. Gelation could also be performed in combination with externally applied deforming forces to obtain gel particles with user-defined shapes. This capability is illustrated in Figure 2d, which shows various shapes were generated by applying deforming forces at the same time that gelation was induced.

In summary, the results in Figure 2 demonstrate several points. First, the semipermeable PEM retains the high-molecular mass chitosan within the capsule but allows externally imposed stimuli to be transmitted into this compartment to induce chitosan's spatially localized self-assembly. Second, the localized sol−gel transition yields capsules with altered mechanical (i.e., elastic) properties. Third, the results are consistent with the gels being the result of strong noncovalent interactions: the size and shape of the gelled capsules depend on the forces exerted on the capsule at the time that gelation is induced.

Creating Complex Internal Structure. Previous investigators have shown that complex multilayer structures can be generated when gel-inducing stimuli are applied intermittently (e.g., to interrupt the gelation process).[15−18] Here, we examined if a sequence of externally imposed stimuli could generate complex internal structures within the capsule. Specifically, we prepared capsules containing chitosan solutions and exposed these capsules to a sequence of gel-inducing (5% NaOH) and noninducing (water) conditions as illustrated in Figure 3. During each step, we collected photomicrographs to show the structure emerging within the capsule.

The initial image at the left in Figure 3 is for the initial fluid-filled capsule. This capsule was then immersed in base for 30 s to induce gelation of the encapsulated chitosan solution. As illustrated by the second image in Figure 3, a chitosan gel layer began growing from the membrane's inner surface into the capsule interior. Importantly, this image indicates that chitosan's gelation does not occur homogeneously throughout the capsule but appears to be localized to the outer region of the capsule. This observation is consistent with previous investigations that show chitosan's gelation occurs as a front and this gelation front is colocalized with the pH neutralization front.[19,20] Presumably, the base that diffuses from the external

dx.doi.org/10.1021/am405544r | ACS Appl. Mater. Interfaces 2014, 6, 2948−2957

solution through the capsule membrane rapidly neutralizes chitosan and induces this polysaccharide's gelation.

After this initial base incubation, the partially gelled capsule was transferred to water for 30 s, and an image was collected during this incubation. The third image in Figure 3 shows a second chitosan gel layer began forming during this water incubation. This observation is somewhat surprising; presumably, some base had been retained in the initial chitosan gel layer and diffuses into the capsule to induce gelation of this second layer. The partially gelled capsule with two layers was returned to the base solution and incubated for an additional 30 s. The next image in Figure 3 indicates that a third gel layer had formed during this base treatment. Two further treatments, one with water and one with base, yielded additional chitosan gel layers.

In summary, the *in situ* observations during the gel-forming sequence shown in Figure 3 demonstrate that a complex internal multilayer structure can be generated in response to a sequence of externally imposed stimuli. As noted, others have observed that stimulus-responsive gel-forming biopolymers can form multilayer structures, although this phenomenon in not completely understood.[15−18]

To assess how the gel-inducing sequence affects the microstructure of the gelled compartment, we prepared capsules, gelled them under different conditions, freeze-dried the gelled capsules, and then examined their cross-sectional structures using SEM. The structure in Figure 4a was obtained from a capsule that was gelled in 5% NaOH for 10 min. This condition led to the formation of a single gel layer inside the capsule. The capsule in Figure 4b was gelled by alternatively incubating it in 5% NaOH (for 2 min) and water (for 2 min) and then repeating this sequence for a total of three cycles (a total of six incubation steps). The cross section of this gelled capsule shows six separate gel layers. A third capsule was gelled by alternatively incubating it in 2.5% NaOH (for 1 min) and water (for 1 min) for a total of eight cycles (16 incubations). Figure 4c shows that this sequential treatment leads to well-defined multilayer structures within the capsule. A final capsule was gelled using lower base concentrations in a sequence of incubations in 0.5% NaOH (for 1 min) and water (for 1 min) for a total of 15 cycles (30 incubations). Figure 4d shows thin multilayers were formed in response to this gel-inducing sequence.

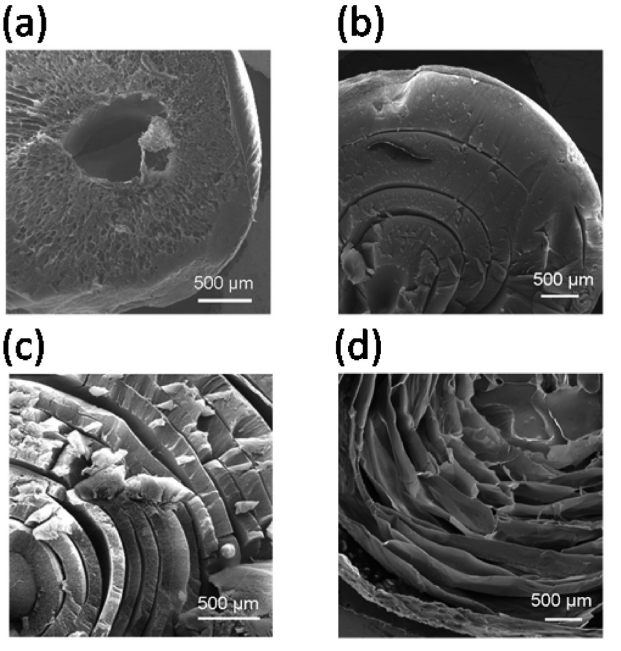

Figure 4. Cross-sectional microstructure of gelled capsules observed by SEM. (a) Gelation induced by a single step, immersion in 5% NaOH for 10 min. (b) Gelation induced by a sequence of three cycles in which each cycle involved immersion in 5% NaOH for 2 min and then in water for 2 min. (c) Gelation induced by a sequence of eight cycles in which each cycle involved immersion in 2.5% NaOH for 1 min and then in water for 1 min. (d) Gelation induced by a sequence of 15 cycles in which each cycle involved immersion in 0.5% NaOH for 1 min and then in water for 1 min.

Controlling Multilayer Structure. The previous figures demonstrate that multilayers can be generated within the capsule by imposing a sequence of external stimuli that induce gelation. While the mechanistic details of this phenomenon may be unclear, we examined the ability to control multilayer structure by controlling the imposed stimuli. The schematic in Figure 5a illustrates our experimental approach. We began by forming a capsule and induced multilayer formation by sequentially transferring it to a base and then to water. One variable changed in the experiment was the time that the capsule was incubated in each solution ($Time_{soak}$; within an individual experiment, this time was the same for every step in the sequence). The second variable that changed was the concentration of base NaOH. After each capsule had been fully gelled, the internal structure was imaged using a stereomicroscope, the number of layers was counted, and the layer thicknesses were measured.

The results in Figure 3 indicate that each transfer step (between base and water or water and base) yields a gel layer; thus, two layers are expected for each cycle shown in Figure 5a. The results in Figure 5b demonstrate such a linear increase in the number of multilayers formed until the contents of the capsule have been completely gelled (illustrated by the dashed lines in Figure 5b). After the capsule has been fully gelled, further transfers do not have an obvious effect on the internal structure (i.e., the number of layers and their thickness do not change). Importantly, Figure 5b shows that this procedure allows a large number of multilayers to be generated within the capsule compartment.

Because gel formation results from the diffusion of base into the capsule, two additional expectations can be envisioned for this experiment. First, if the soaking time is extended to allow more time for base diffusion, then the gel layers would be expected to become thicker. Figure 5c demonstrates this expectation. The second expectation is that if the base concentration is increased, its diffusion should be accelerated and the individual gel layers should be thicker. Figure 5d demonstrates this second expectation.

In summary, the results in Figure 5 demonstrate that the number of multilayers and their thickness can be controlled by the sequence of external stimuli used to trigger gel formation.

Multilayer as a Template for Hard Matter. To illustrate the potential utility of the multilayer hydrogel structure, we examined its ability to serve as a structurally complex template using the sequence of steps outlined in Figure 6a. As indicated, multilayer hydrogel templates were created and then incubated for 24 h in a 1:1 (by volume) ethanol/water solution containing $FeCl_2$ (final concentration of 0.5 M). Visually, these templates were observed to become brownish during this step. After the $FeCl_2$ incubation, the templates were then transferred to a basic

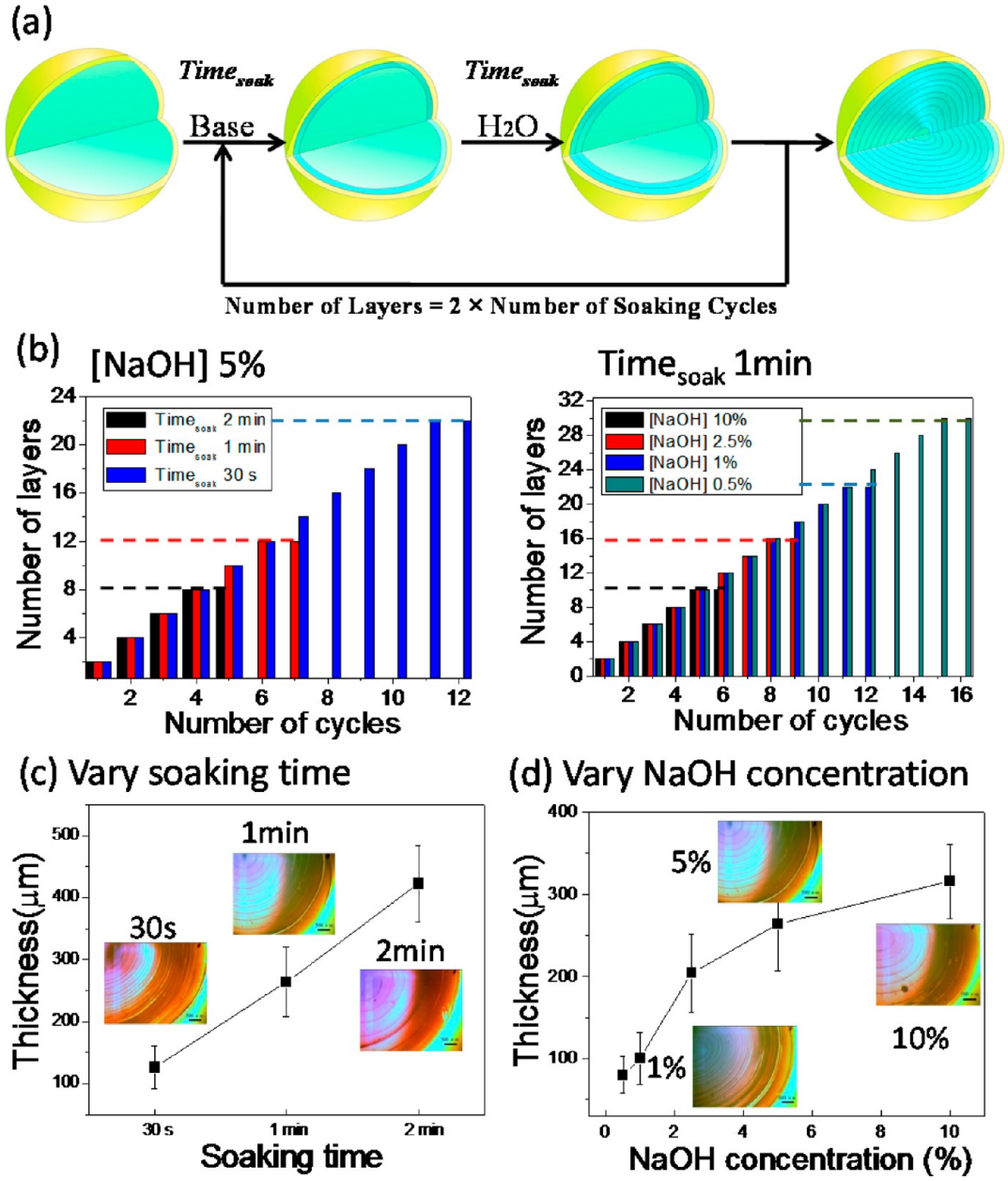

Figure 5. Controlling multilayer structure by controlling the sequence of externally imposed cues. (a) Schematic illustrating multilayer formation in response to the repetitive transfer of the capsule between water and base. (b) Results indicate that each transfer step yields a layer (note there are two transfer steps per cycle) until the capsule has been completely gelled (the dashed horizontal lines indicate when the capsules have been completely gelled for the different conditions). (c) Results indicate that the thickness of each gel layer is increased by the incubation time for each step (i.e., $Time_{soak}$). (d) Results indicate that the thickness of each gel layer is increased by the concentration of base. Note that insets in panels c and d are photomicrographs of multilayer gels.

solution (2 M NaOH) and incubated for 20 min, at which time they became black presumably because of the formation of iron hydroxide. The template particles were then collected and freeze-dried (−30 °C for 8 h), after which they were observed to be considerably harder and somewhat brittle. Some of these template particles were purposefully broken to reveal the underlying structure as shown by the representative images in Figure 6b.

Freeze-dried template particles were then placed in a tube furnace, and the temperature was increased at a rate of 2 °C/min to a final temperature of 600 °C, where it was held for 4 h and then allowed to cool overnight. The images in Figure 6c show the intact particles formed from this calcination treatment. After heat treatment, the particles were very brittle and could be easily broken to reveal their internal structure. The photos in Figure 6d show that a multilayer structure had been templated into the iron oxide particles.

In addition to the multilayer hydrogel template, we prepared two controls for this study. One control template was an ungelled capsule (i.e., a chitosan solution was in the capsule core). The other control template was a gelled capsule with a single gelled layer in the core. Both control templates were processed using the steps in Figure 6a. The photographs in Figure 6e show that the iron oxide particles generated from these control templates lack the complex internal structure

dx.doi.org/10.1021/am405544r | ACS Appl. Mater. Interfaces 2014, 6, 2948−2957

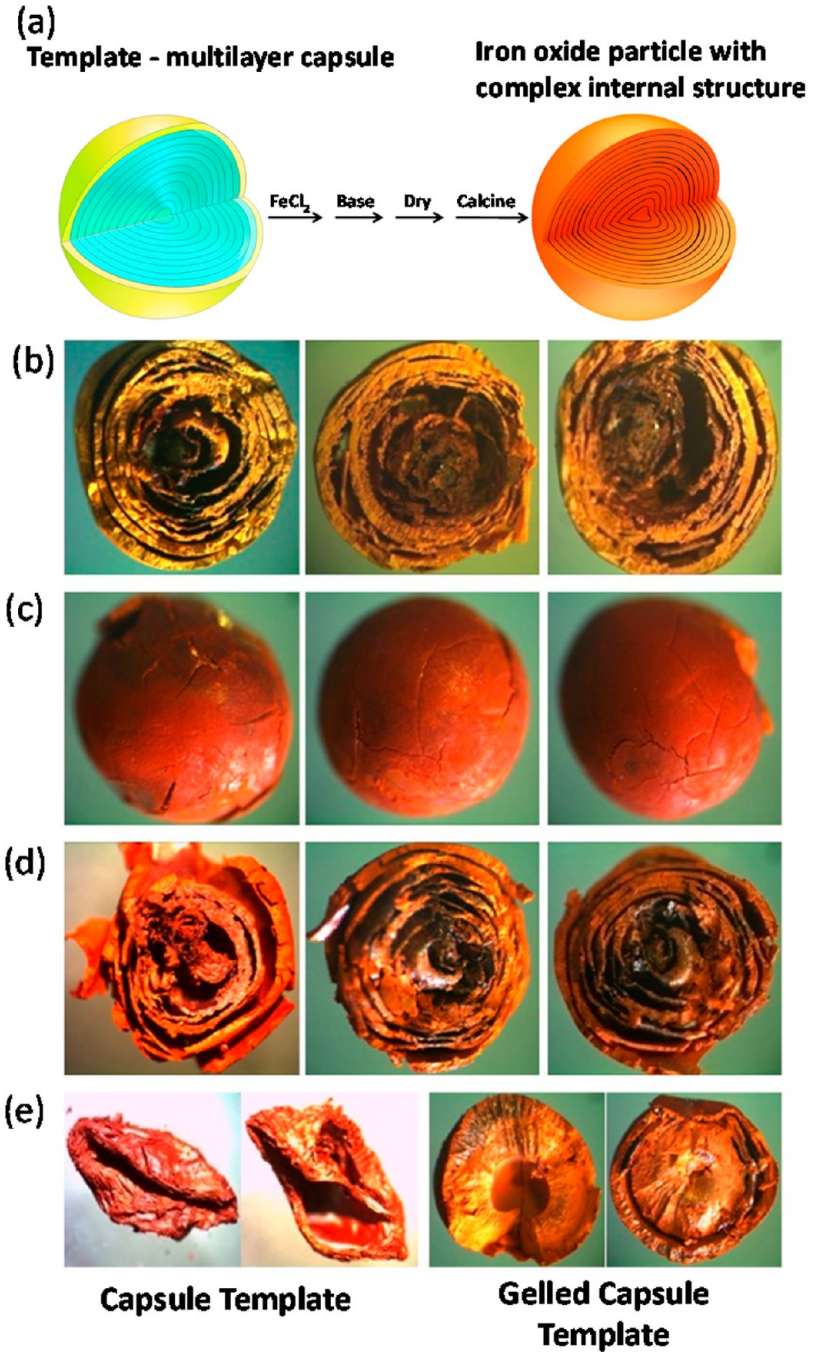

Figure 6. Soft templates for creating hard particles with a complex internal structure. (a) Schematic illustrating the iron oxide templating procedure. (b) Photographs of multimembrane templates before calcination. (c) Photographs of intact iron oxide particles generated from the multimembrane template. (d) Photographs revealing the internal structure of iron oxide particles generated from the multimembrane template. (e) Photographs of structure generated from the control templates that lacked the multimembrane structure.

compared to the particles generated from the multilayer template.

The iron oxide particles were characterized by three different techniques. First, the morphology of the oxide particles was observed by a field emission scanning electron microscope (FE-SEM). The images in Figure 7a show that the oxide particles have a plate shape with a diameter of 30−50 nm and a thickness of 5−10 nm. The shapes of these oxide particles differ from those of nanoparticles prepared from commonly used coprecipitation methods in which the oxide particles possess a needle shape.[21,22] Presumably, the multilayer hydrogel provides accommodations for the nanoplates to grow.

Second, the crystal type of the iron oxide particles was examined by X-ray diffraction (XRD). Figure 7b shows a typical X-ray diffraction of iron oxide particles. It is evident that all of the diffraction peaks are in good agreement with the reference JCPDS Card 33-0664. No diffraction peaks are evident for Fe_3O_4, β-Fe_2O_3, or other iron precursors. The sharp diffraction peaks indicate that the iron oxide particles are highly crystallized α-Fe_2O_3.

dx.doi.org/10.1021/am405544r | ACS Appl. Mater. Interfaces 2014, 6, 2948−2957

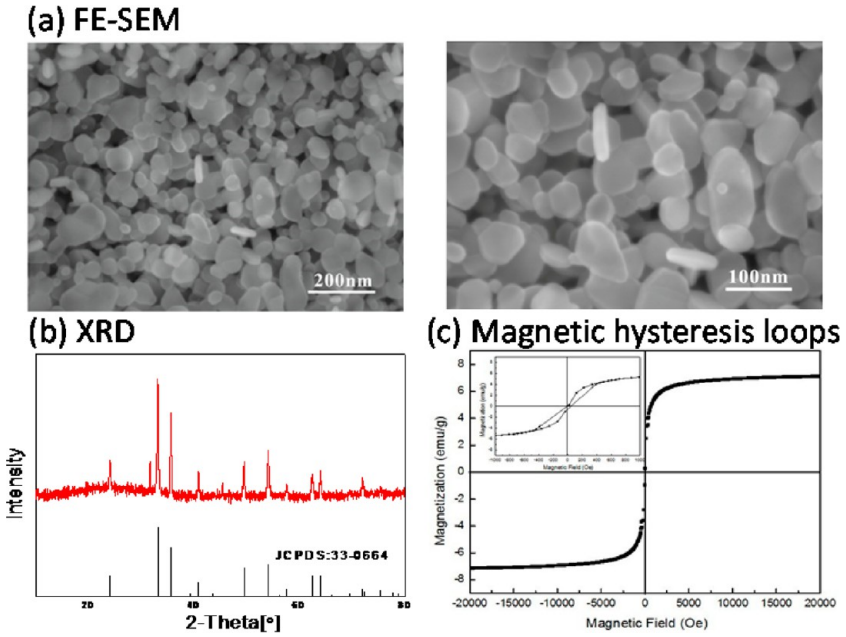

Figure 7. Characterization of the templated iron oxide. (a) FE-SEM images of iron oxide nanoparticles with different magnifications. (b) XRD pattern of iron oxide particles with comparison to the reference JCPDS Card. (c) Magnetic hysteresis loops of iron oxide particles.

Finally, the magnetic properties of α-Fe_2O_3 particles were characterized by magnetic hysteresis measurements. As shown in Figure 7c, the plate-shaped iron oxide particles exhibit weak ferromagnetic behaviors with a small hysteresis loop and coercivity. Potentially, the ability to fabricate α-Fe_2O_3 nanoplates may be useful for various applications of α-Fe_2O_3 in biotechnology, catalysis, and batteries.[23−26] Importantly, the results from this study indicate that the templated synthesis method allows these nanomaterials to be organized into complex macroscale structures.

DISCUSSION

In this study, we first localize the pH-responsive aminopolysaccharide chitosan within a membranous capsule formed by complexation of the weak polyelectrolytes chitosan and alginate. Polymer membranes generated by either electrostatic[13,14,27] or hydrogen bond[28,29] complexation are simple to form and versatile and can be further modified to confer various additional capabilities. Currently, there is considerable effort to create capsules[30] with greater internal complexity (e.g., multiple compartments)[31−34] and/or with stimulus-responsive membranes (e.g., for controlled release).[35−42] In this study, our polyelectrolyte membrane (PEM) is used to compartmentalize contents that are stimulus-responsive and can respond to external stimuli to generate complex internal structure (i.e., multilayers).

The chitosan within our capsule is triggered to undergo a localized sol−gel transition in response to an externally imposed increase in pH. This sol−gel transition can be viewed as a self-assembling process involving strong noncovalent interactions[5,43] or a stimulus-triggered manipulation of polymer structure.[44] In either case, this transition converts the contents of the capsule from a solution to a gel with an associated change in mechanical properties (i.e., the contents undergo a transition to a soft solid). As such, this system possesses the characteristics of a chemomechanical sensor−actuator system in which the external chemical cues induce a localized change in mechanical properties.[45,46]

It is believed that chitosan's physical (i.e., noncovalent) gel results from the hydrogen bonds and hydrophobic interactions associated with the crystalline network junctions that serve as the noncovalent cross-links.[47,48] Presumably, these crystalline network junctions are composed of a large number of such weak interactions that cumulatively yield a strong noncovalent bond. Once the chitosan hydrogel is formed, its shape and structure are "locked" in place and the gel does not spontaneously "anneal" to a thermodynamically more stable state within the typical laboratory time scale (i.e., weeks). Because gels are formed from such strong noncovalent interactions, it is possible to impose a shape by exerting deforming forces on the capsule at the same time that gelation is induced by the pH increase. This approach to imposing shape to soft particles offers an alternative to existing methods of imposing shape by using a template (e.g., for layer-by-layer self-assembly)[49,50] or by top-down methods (e.g., molding).[14,51] Obviously, more work is required to evaluate how, and if, appropriate deforming forces could be imposed on these capsules to impart structure at the microscales (e.g., by applying forces through microfluidics or AFM). We should also note that by using biological polymers that undergo reversible sol−gel transitions, the imposed shape and/or structure can be "erased" (e.g., by lowering the pH and redissolving the chitosan).

We believe the most impressive observation of this study is that an externally imposed sequence of stimuli can generate a particle with a complex internal structure (i.e., Figures 3 and 4). This internal multilayer structure can be controlled as evidenced by Figure 5. Polysaccharide hydrogel multilayer structures have been observed previously[52,53] and in our case result from an interruption in the gelation process, although the underlying mechanism of how such an interruption in the gel-inducing stimuli leads to multilayer structure remains unclear.[15−18] We show that this multimembrane particle can serve as a template for the generation of hard matter with a complex internal structure (Figure 6). Interestingly, the use of a soft matter template to organize hard matter can be juxtaposed with the more common use of hard matter to template soft

matter (e.g., the use of silica[38,54−56] or carbonate[31,33] particles as templates for layer-by-layer self-assembly).

Finally, we should note that our methods for creating the complex shape and/or structure rely on the smart properties of biopolymers and controlling the cues that trigger their self-assembly; thus, our methods are simple, rapid, and reagentless (except for the base). Because both chitosan and alginate are commonly ingested, it is expected that these materials should be safe and potentially even edible. Importantly, chitosan and alginate are not unique, and a variety of common biological polymers (e.g., gelatin, agarose, and pectin) can undergo reversible sol−gel transitions; these may provide alternative materials for biofabricating soft matter with complex shapes and internal structures.

EXPERIMENTAL SECTION

Chitosan from crab shells (85% deacetylation and 200 kDa, as reported by the supplier) was purchased from Sigma-Aldrich. Alginate sodium (viscosity of 10 g/L above 0.02 Pa s^{-1}) was purchased from Sinopharm Chemical Reagent Co., Ltd. (Shanghai, China). Dextran Blue (2000 kDa) was purchased from Biosharp. Iron chloride tetrahydrate ($FeCl_2{\cdot}4H_2O$) was purchased from DaMao Chemical Reagent Co. All other reagents were of analytical grade and were used without further purification.

Capsules were prepared using two solutions: chitosan (4%) dissolved in 2% acetic acid and alginate sodium (2%) dissolved in water. Capsules were formed by dropping the chitosan solution into the alginate solution and then incubating the mixture for 4 h to allow the PEM to form. Capsules were removed from the alginate solution and rinsed with water. To facilitate visualization, some capsules were prepared by adding dextran blue (0.1%) to the chitosan solution prior to forming the PEM.

Capsules containing chitosan solutions were gelled by immersion in base solutions. The multilayer chitosan hydrogels were formed by sequentially immersing the PEM capsule in a NaOH solution and water. The concentration of NaOH was varied from 0.1 to 10%, and the time for each incubation was also varied from 30 s to 2 min. The formation of the layer was observed using a stereomicroscope (SZM45, Shunyu, Jiangsu, China). The number of layers was counted and their thickness measured from the optical image by using Nano Measurer software (http://nano-measurer.software.informer.com/). Chemical analyses were performed using FT-IR (Nicolet 5700), XRD (X'Pert Pro, PANalytical), and XPS (KRATOS XSAM800). Mechanical measurements were taken in triplicate using a Texture Analyzer (Stable Micro Systems, UK, with the Texture Expert software) at a compression speed of 2 mm/s to 90% stain.

A multilayer gelled capsule was used as a template for iron oxide particles by incubating the multilayer gelled capsule in a 50% ethanol/water solution containing 0.5 M $FeCl_2$ for 24 h. After the $FeCl_2$ incubation, the multilayer hydrogels were then transferred to a basic solution (2 M NaOH) and incubated for 20 min. The template hydrogels were then collected and freeze-dried (−30 °C for 8 h). The cross section and surface of hydrogels were observed with a stereomicroscope. To remove the template hydrogel, the freeze-dried template particles were placed in a tube furnace and the temperature was increased at a rate of 2 °C/min to a final temperature of 600 °C and held for 4 h. The morphologies of the iron oxide particles were observed by a field emission scanning electronic microscope (ULTRA PLUS, Carl Zeiss AG). The crystal type of the iron oxide particles was examined by a XRD diffractometer (X'Pert Pro, PANalytical). The patterns with Cu Kα radiation were recorded in the region of 2θ from 10° to 80° at a rate of 4°/min. Magnetic properties were investigated using a Physical Property Measurement System (9T, Quantum Design).

AUTHOR INFORMATION

Corresponding Authors

*E-mail: shixwwhu@163.com. Phone: +86-27-68778501.
*E-mail: gpayne@umd.edu. Phone: (301) 405-8389.

Notes

The authors declare no competing financial interest.

ACKNOWLEDGMENTS

We gratefully acknowledge the financial support from the National Natural Science Foundation of China (Grants 21007049, 51373124, and 21334005), the High-end Foreign Experts Program (GDW20134200126), the Robert W. Deutsch Foundation, and the U.S. Department of Defense (DTRA BO085PO008).

REFERENCES

(1) Richtering, W.; Pich, A. The special behaviours of responsive core-shell nanogels. *Soft Matter* **2012**, *8* (45), 11423−11430.
(2) Stuart, M. A.; Huck, W. T.; Genzer, J.; Muller, M.; Ober, C.; Stamm, M.; Sukhorukov, G. B.; Szleifer, I.; Tsukruk, V. V.; Urban, M.; Winnik, F.; Zauscher, S.; Luzinov, I.; Minko, S. Emerging applications of stimuli-responsive polymer materials. *Nat. Mater.* **2010**, *9* (2), 101−113.
(3) O'Leary, L. E. R.; Fallas, J. A.; Bakota, E. L.; Kang, M. K.; Hartgerink, J. D. Multi-hierarchical self-assembly of a collagen mimetic peptide from triple helix to nanofibre and hydrogel. *Nat. Chem.* **2011**, *3* (10), 821−828.
(4) Chung, W. J.; Oh, J. W.; Kwak, K.; Lee, B. Y.; Meyer, J.; Wang, E.; Hexemer, A.; Lee, S. W. Biomimetic self-templating supramolecular structures. *Nature* **2011**, *478* (7369), 364−368.
(5) Rybtchinski, B. Adaptive Supramolecular Nanomaterials Based on Strong Noncovalent Interactions. *ACS Nano* **2011**, *5* (9), 6791−6818.
(6) Moore, J. S.; Kraft, M. L. Chemistry: Synchronized self-assembly. *Science* **2008**, *320* (5876), 620−621.
(7) Velichko, Y. S.; Mantei, J. R.; Bitton, R.; Carvajal, D.; Shull, K. R.; Stupp, S. I. Electric Field Controlled Self-Assembly of Hierarchically Ordered Membranes. *Adv. Funct. Mater.* **2012**, *22* (2), 369−377.
(8) Correia, C. R.; Sher, P.; Reis, R. L.; Mano, J. F. Liquified chitosan-alginate multilayer capsules incorporating poly(L-lactic acid) microparticles as cell carriers. *Soft Matter* **2013**, *9* (7), 2125−2130.
(9) Sorlier, P.; Denuziere, A.; Viton, C.; Domard, A. Relation between the degree of acetylation and the electrostatic properties of chitin and chitosan. *Biomacromolecules* **2001**, *2* (3), 765−772.
(10) Cheng, Y.; Gray, K. M.; David, L.; Royaud, I.; Payne, G. F.; Rubloff, G. W. Characterization of the cathodic electrodeposition of semicrystalline chitosan hydrogel. *Mater. Lett.* **2012**, *87*, 97−100.
(11) Lawrie, G.; Keen, I.; Drew, B.; Chandler-Temple, A.; Rintoul, L.; Fredericks, P.; Grondahl, L. Interactions between alginate and chitosan biopolymers characterized using FTIR and XPS. *Biomacromolecules* **2007**, *8* (8), 2533−2541.
(12) van Hoogmoed, C. G.; Busscher, H. J.; de Vos, P. Fourier transform infrared spectroscopy studies of alginate-PLL capsules with varying compositions. *J. Biomed. Mater. Res., Part A* **2003**, *67* (1), 172−178.
(13) Capito, R. M.; Azevedo, H. S.; Velichko, Y. S.; Mata, A.; Stupp, S. I. Self-assembly of large and small molecules into hierarchically ordered sacs and membranes. *Science* **2008**, *319* (5871), 1812−1816.
(14) Mendes, A. C.; Smith, K. H.; Tejeda-Montes, E.; Engel, E.; Reis, R. L.; Azevedo, H. S.; Mata, A. Co-Assembled and Microfabricated Bioactive Membranes. *Adv. Funct. Mater.* **2013**, *23* (4), 430−438.
(15) Ladet, S.; David, L.; Domard, A. Multi-membrane hydrogels. *Nature* **2008**, *452* (7183), 76−79.
(16) Ladet, S. G.; Tahiri, K.; Montembault, A. S.; Domard, A. J.; Corvol, M. T. M. Multi-membrane chitosan hydrogels as chondrocytic cell bioreactors. *Biomaterials* **2011**, *32* (23), 5354−5364.

(17) Dai, H. J.; Li, X. F.; Long, Y. H.; Wu, J. J.; Liang, S. M.; Zhang, X. L.; Zhao, N.; Xu, J. Multi-membrane hydrogel fabricated by facile dynamic self-assembly. *Soft Matter* **2009**, *5* (10), 1987−1989.
(18) Yan, K.; Ding, F.; Bentley, W. E.; Deng, H.; Du, Y.; Payne, G. F.; Shi, X.-W. Coding for hydrogel organization through signal guided self-assembly. *Soft Matter* **2014**, *10* (3), 465−469.
(19) Cheng, Y.; Luo, X. L.; Betz, J.; Buckhout-White, S.; Bekdash, O.; Payne, G. F.; Bentley, W. E.; Rubloff, G. W. In situ quantitative visualization and characterization of chitosan electrodeposition with paired sidewall electrodes. *Soft Matter* **2010**, *6* (14), 3177−3183.
(20) Dobashi, T.; Tomita, N.; Maki, Y.; Chang, C. P.; Yamamoto, T. An analysis of anisotropic gel forming process of chitosan. *Carbohydr. Polym.* **2011**, *84* (2), 709−712.
(21) Nunez, N. O.; Morales, M. P.; Tartaj, P.; Serna, C. J. Preparation of high acicular and uniform goethite particles by a modified-carbonate route. *J. Mater. Chem.* **2000**, *10* (11), 2561−2565.
(22) Nunez, N. O.; Tartaj, P.; Morales, M. P.; Gonzalez-Carreno, T.; Serna, C. J. Correlation between microstructural features and magnetic behavior of Fe-based metallic nanoneedles. *Acta Mater.* **2006**, *54* (1), 219−224.
(23) Kosa, S. A.; Maksod, I. H. A. E.; Alkhateeb, L.; Hegazy, E. Z. Preparation and surface characterization of CuO and Fe_2O_3 catalyst. *Appl. Surf. Sci.* **2012**, *258* (19), 7617−7624.
(24) Tartaj, P. Nanomagnets: From fundamental physics to biomedicine. *Curr. Nanosci.* **2006**, *2* (1), 43−53.
(25) Qu, J.; Yin, Y.-X.; Wang, Y.-Q.; Yan, Y.; Guo, Y.-G.; Song, W.-G. Layer Structured α-Fe_2O_3 Nanodisk/Reduced Graphene Oxide Composites as High-Performance Anode Materials for Lithium-Ion Batteries. *ACS Appl. Mater. Interfaces* **2013**, *5* (9), 3932−3936.
(26) Frank, J. A.; Miller, B. R.; Arbab, A. S.; Zywicke, H. A.; Jordan, E. K.; Lewis, B. K.; Bryant, L. H.; Bulte, J. W. M. Clinically applicable labeling of mammalian and stem cells by combining; Superparamagnetic iron oxides and transfection agents. *Radiology* **2003**, *228* (2), 480−487.
(27) Carvajal, D.; Bitton, R.; Mantei, J. R.; Velichko, Y. S.; Stupp, S. I.; Shull, K. R. Physical properties of hierarchically ordered self-assembled planar and spherical membranes. *Soft Matter* **2010**, *6* (8), 1816−1823.
(28) Such, G. K.; Johnston, A. P. R.; Caruso, F. Engineered hydrogen-bonded polymer multilayers: From assembly to biomedical applications. *Chem. Soc. Rev.* **2011**, *40* (1), 19−29.
(29) Kozlovskaya, V.; Kharlampieva, E.; Drachuk, I.; Cheng, D.; Tsukruk, V. V. Responsive microcapsule reactors based on hydrogen-bonded tannic acid layer-by-layer assemblies. *Soft Matter* **2010**, *6* (15), 3596−3608.
(30) Tong, W. J.; Song, X. X.; Gao, C. Y. Layer-by-layer assembly of microcapsules and their biomedical applications. *Chem. Soc. Rev.* **2012**, *41* (18), 6103−6124.
(31) Kreft, O.; Prevot, M.; Mohwald, H.; Sukhorukov, G. B. Shell-in-shell microcapsules: A novel tool for integrated, spatially confined enzymatic reactions. *Angew. Chem., Int. Ed.* **2007**, *46* (29), 5605−5608.
(32) Delcea, M.; Yashchenok, A.; Videnova, K.; Kreft, O.; Mohwald, H.; Skirtach, A. G. Multicompartmental Micro- and Nanocapsules: Hierarchy and Applications in Biosciences. *Macromol. Biosci.* **2010**, *10* (5), 465−474.
(33) Shi, J. F.; Zhang, L.; Jiang, Z. Y. Facile Construction of Multicompartment Multienzyme System through Layer-by-Layer Self-Assembly and Biomimetic Mineralization. *ACS Appl. Mater. Interfaces* **2011**, *3* (3), 881−889.
(34) Lee, H. Y.; Tiwari, K. R.; Raghavan, S. R. Biopolymer capsules bearing polydiacetylenic vesicles as colorimetric sensors of pH and temperature. *Soft Matter* **2011**, *7* (7), 3273−3276.
(35) Huang, X.; Appelhans, D.; Formanek, P.; Simon, F.; Voit, B. Tailored Synthesis of Intelligent Polymer Nanocapsules: An Investigation of Controlled Permeability and pH-Dependent Degradability. *ACS Nano* **2012**, *6* (11), 9718−9726.
(36) Bird, R.; Freemont, T.; Saunders, B. R. Tuning the properties of pH-responsive and redox sensitive hollow particles and gels using copolymer composition. *Soft Matter* **2012**, *8* (4), 1047−1057.
(37) Kozlovskaya, V.; Zavgorodnya, O.; Wang, Y.; Ankner, J. F.; Kharlampieva, E. Tailoring Architecture of Nanothin Hydrogels: Effect of Layering on pH-Triggered Swelling. *ACS Macro Lett.* **2013**, *2* (3), 226−229.
(38) Ye, C. H.; Drachuk, I.; Calabrese, R.; Dai, H. Q.; Kaplan, D. L.; Tsukruk, V. V. Permeability and Micromechanical Properties of Silk Ionomer Microcapsules. *Langmuir* **2012**, *28* (33), 12235−12244.
(39) Ye, C. H.; Shchepelina, O.; Calabrese, R.; Drachuk, I.; Kaplan, D. L.; Tsukruk, V. V. Robust and Responsive Silk Ionomer Microcapsules. *Biomacromolecules* **2011**, *12* (12), 4319−4325.
(40) Zhu, Y.; Tong, W. J.; Gao, C. Y. Molecular-engineered polymeric microcapsules assembled from Concanavalin A and glycogen with specific responses to carbohydrates. *Soft Matter* **2011**, *7* (12), 5805−5815.
(41) Becker, A. L.; Zelikin, A. N.; Johnston, A. P. R.; Caruso, F. Tuning the Formation and Degradation of Layer-by-Layer Assembled Polymer Hydrogel Microcapsules. *Langmuir* **2009**, *25* (24), 14079−14085.
(42) Cui, J.; Yan, Y.; Such, G. K.; Liang, K.; Ochs, C. J.; Postma, A.; Caruso, F. Immobilization and Intracellular Delivery of an Anticancer Drug Using Mussel-Inspired Polydopamine Capsules. *Biomacromolecules* **2012**, *13* (8), 2225−2228.
(43) Yu, G.; Yan, X.; Han, C.; Huang, F. Characterization of supramolecular gels. *Chem. Soc. Rev.* **2013**, *42*, 6697−6722.
(44) Zhang, J.; Li, X.; Li, X. Stimuli-triggered structural engineering of synthetic and biological polymeric assemblies. *Prog. Polym. Sci.* **2012**, *37* (8), 1130−1176.
(45) Kato, K.; Schneider, H. J. Supramolecular Interactions in Chitosan Gels. *Eur. J. Org. Chem.* **2009**, *7*, 1042−1047.
(46) Schneider, H.-J.; Strongin, R. M. Supramolecular Interactions in Chemomechanical Polymers. *Acc. Chem. Res.* **2009**, *42* (10), 1489−1500.
(47) Popa-Nita, S.; Alcouffe, P.; Rochas, C.; David, L.; Domard, A. Continuum of Structural Organization from Chitosan Solutions to Derived Physical Forms. *Biomacromolecules* **2010**, *11* (1), 6−12.
(48) Popa-Nita, S.; Rochas, C.; David, L.; Domard, A. Structure of Natural Polyelectrolyte Solutions: Role of the Hydrophilic/Hydrophobic Interaction Balance. *Langmuir* **2009**, *25* (11), 6460−6468.
(49) Kozlovskaya, V.; Higgins, W.; Chen, J.; Kharlampieva, E. Shape switching of hollow layer-by-layer hydrogel microcontainers. *Chem. Commun.* **2011**, *47* (29), 8352−8354.
(50) Kozlovskaya, V.; Wang, Y.; Higgins, W.; Chen, J.; Chen, Y.; Kharlampieva, E. pH-triggered shape response of cubical ultrathin hydrogel capsules. *Soft Matter* **2012**, *8* (38), 9828−9839.
(51) Merkel, T. J.; Herlihy, K. P.; Nunes, J.; Orgel, R. M.; Rolland, J. P.; DeSimone, J. M. Scalable, Shape-Specific, Top-Down Fabrication Methods for the Synthesis of Engineered Colloidal Particles. *Langmuir* **2010**, *26* (16), 13086−13096.
(52) Duan, J. J.; Hou, R. X.; Xiong, X. P.; Wang, Y. D.; Wang, Y.; Fu, J.; Yu, Z. J. Versatile fabrication of arbitrarily shaped multi-membrane hydrogels suitable for biomedical applications. *J. Mater. Chem. B* **2013**, *1* (4), 485−492.
(53) Dhanasingh, A.; Groll, J. Polysaccharide based covalently linked multi-membrane hydrogels. *Soft Matter* **2012**, *8* (5), 1643−1647.
(54) Ochs, C. J.; Hong, T.; Such, G. K.; Cui, J.; Postma, A.; Caruso, F. Dopamine-Mediated Continuous Assembly of Biodegradable Capsules. *Chem. Mater.* **2011**, *23* (13), 3141−3143.
(55) Postma, A.; Yan, Y.; Wang, Y.; Zelikin, A. N.; Tjipto, E.; Caruso, F. Self-Polymerization of Dopamine as a Versatile and Robust Technique to Prepare Polymer Capsules. *Chem. Mater.* **2009**, *21* (14), 3042−3044.
(56) Shimoni, O.; Yan, Y.; Wang, Y. J.; Caruso, F. Shape-Dependent Cellular Processing of Polyelectrolyte Capsules. *ACS Nano* **2013**, *7* (1), 522−530.